A Differential Slot-type Dual-polarization Ultra-wideband Antenna

Zhao Neng Jiang[1,2], Zhi Xin Wang[1], Xiao Feng Xuan[1], Li Ying Nie[1], and Ye Jiang[1]

[1]Department of Information Engineering
Hefei University of Technology, Hefei, 230009, China

[2]National Mobile Communications Research Laboratory
Southeast University, Jiangsu, 210096, China
liyingnie@sina.com

Abstract – A differentially fed dual-polarization slotted antenna with an ultra-wide bandwidth and low cross polarization is presented in this paper. The antenna is composed of a radiation patch and a ground plane, both of which are printed on the top of the dielectric substrate. The ground is extended toward the radiation patch to form a slotted coplanar structure. In order to expand the bandwidth, a cross-shape symmetrical slotted structure is loaded into the radiation patch. Differential feed is adopted to realize 0°/90° linear polarizations and suppress the cross polarization. Simulation and measurement results show that the proposed antenna with dimensions of $0.53\lambda_0 \times 0.53\lambda_0 \times 0.0135\lambda_0$ (λ_0 is the wavelength at 4 GHz) has a differential mode impedance bandwidth of 82.25% (2.27-5.56 GHz), a differential feed port isolation of higher than 28 dB, and a cross polarization level of less than -30 dB, which achieves the characteristics of ultra-wideband, high isolation, and low cross polarization level.

Index Terms – coplanar waveguide, differential feed, dual polarization, low-profile, ultra-wideband.

I. INTRODUCTION

With the development of wireless technology in the fields of personal communication and military applications, people have higher and higher requirements for the design of communication system antennas under the limited spectrum resources [1]. In order to reduce the influence of multipath effect and increase the channel capacity of the system, dual-polarization antenna arises at the right moment [2]. Moreover, dual-polarization antenna can be broadband, compatible with a variety of communication standards or support high-speed data transmission, so as to reduce the demand for the number of antennas in a certain operating frequency band. It can also be miniaturized to reduce the carrier space occupation and easy to integrate with the carrier [3–5].

In the implementation of dual-polarization, two independent ports are usually adopted to feed the cross dipole antenna in order to obtain vertical and horizontal polarization modes [6]. Traditional dual-polarization cross-dipole antennas have narrow operating bandwidth and high profile [7–10]. For example, a dual-polarization cross-slotted antenna with two orthogonal groove radiators was designed in [11]. To reduce the antenna size, a small ground was designed with the same length of the hypotenuse as the slot, and inductors were loaded at both ends of the slot. The common impedance bandwidth of the dual-polarization antenna at port 1 and port 2 is 1.56 - 2.73 GHz (54.5%), the isolation is greater than 26 dB, and the profile height is about $0.27\lambda_0$. In [12], a pair of orthogonally-printed dipoles and a reflective ground were used to obtain two linear polarizations. A slot in the center of the dipoles and short connection between the orthogonally-printed dipoles could improve the isolation and cross polarization. The antenna has a cross-polarization of < -30 dB, a port isolation of $>$ 35 dB, and a profile height of $0.15\lambda_{575\text{MHz}}$ within 575 - 722 MHz (22.7%). The antennas described in [11, 12] have complex structure, relatively small bandwidth and a high profile, which makes them difficult to integrate with microwave circuits. In [13], a reflection plate was designed based on the in-phase reflection principle of artificial magnetic conductor (AMC) structure, so that the height of the dual-polarization antenna was reduced by half, and the antenna worked within 1.67 - 2.98 GHz (56%). Although the antenna profile height is reduced, the loading of AMC also makes the antenna structure more complex.

However, a microstrip antenna can obtain two orthogonal polarization modes by feeding different patches on the same dielectric layer or radiation patches on different dielectric layers. The operating frequency band of microstrip antenna can be expanded by adding parasitic elements, etching slots and so on. A dual-polarization planar slotted antenna is proposed in [14], which adopts

different feeding mechanisms of high isolation ports to achieve two kinds of orthogonal polarization. Horizontal polarization is excited by a curved line coupling slot and vertical polarization is fed by a stepped monopole. In [15], a compact dual-polarization slotted antenna is presented, which uses triple-mode stepped slotted-line resonator and dual-mode criss-cross monopole. Through feeding two ports symmetrically at the opposite positions of the slot to achieve orthogonal polarization, the antenna can achieve a wide operating frequency band (1.63 - 2.93 GHz) and a high port isolation ($>$ 32 dB). The antenna described in [14, 15] uses microstrip antenna to achieve dual-polarization, which results in a low-profile height, but the cross-polarization level is not high enough, and the operating bandwidth is still not large enough.

Targeting the deficiencies of narrow bandwidth and poor polarization purity of traditional planar microstrip slotted antenna, a compact ultra-wideband dual-polarization slotted antenna with low cross polarization is proposed in this paper. It consists of a symmetrical radiation patch and a ground plane which form a gap in the upper layer of the dielectric plate. The antenna adopts coplanar waveguide (CPW) structure for differential feed. Differential feed is to feed two ports of the antenna at the same time through two signal lines. The signals fed through these two ports have the characteristics of equal amplitude and reverse phase, so it is also called inverting feed technology. The inverting feed technology can suppress the high-order modes generated on the metal radiation patch. It can counteract the coupling between the same pair of feed probes and the radiation leakage between them, so that the antenna cross polarization can be suppressed and the isolation between the ports can be improved [16]. To further expand the antenna bandwidth, a cross-shape slot is loaded in the center of the radiation patch. Simulation and experimental results show that the overall antenna size is 40 mm × 40 mm × 1.016 mm, the impedance bandwidth can reach 82.25% (2.27 - 5.56 GHz), the port isolation is higher than 28 dB, and the cross-polarization level is less than −30 dB. It can meet the requirements of miniaturization, ultra-wide bandwidth, high isolation, and low cross polarization.

II. ANTENNA DESIGN
A. Antenna structure
Figure 1 shows the geometry of the dual-polarization antenna. The radiator and ground are printed on a 1.016 mm-thickness Rogers 5880 substrate with a relative dielectric constant of 2.2 and a loss tangent of 0.009. The radiation patch is a symmetrical structure composed of four semicircles with a radius of R and two rectangles with a width of k and a length of twice j. To ex-

pand the impedance matching bandwidth, a cross-shape slot with a width of m and a length of twice l is loaded in the center. The end sides of the semicircle are feeder parts with a width of p. The antenna is fed by coplanar waveguide (CPW). The ground extends toward the radiation patch, and an s-width gap is formed. According to the design principle of microstrip antenna, the patch width L can be expressed as:

$$L = \frac{c}{2f_r}\left(\frac{\varepsilon_r+1}{2}\right)^{-\frac{1}{2}}, \qquad (1)$$

where f_r is the resonant frequency, c is the speed of light, and ε_r is the dielectric constant of the substrate. According to equation (1), the width of the patch can be roughly calculated to be at least 30 mm, so $R + j$ should be greater than 15 mm. The design parameters of the final structure are as follows: $W = 40$ mm, $R = 6$ mm, $k = 4$ mm, $j = 11$ mm, $p = 2.4$ mm, $m = 3$ mm, $l = 9.5$ mm, $s = 0.5$ mm.

(a)

(b)
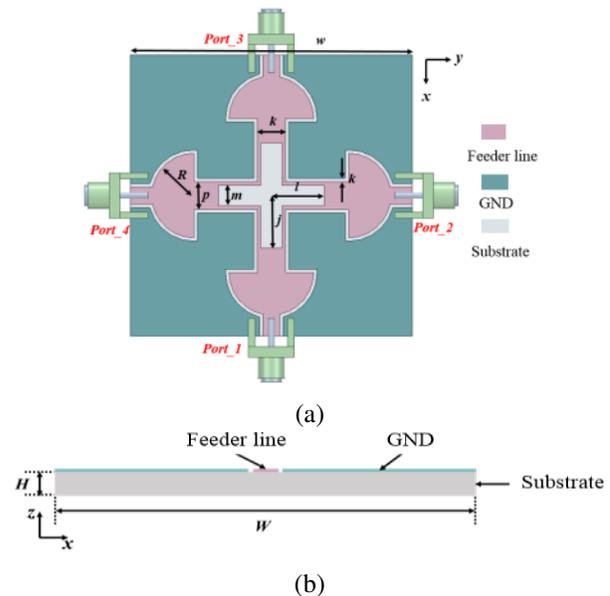
Fig. 1. Geometry of the proposed antenna. (a) Top view. (b) Front view.

The four feed ports of the antenna are shown in Fig. 1. Differential feed port 1 is formed when port_1 and port_3 feed the signal of equal amplitude and reverse phase at the same time, and the antenna will generate vertical polarization mode. When port_2 and port_4 feed equal amplitude and reverse phase signals at the same time, the differential feed port_2 is formed, and the antenna will generate horizontal polarization mode.

B. Design process
The design process of the dual-polarization antenna is shown in Fig. 2. Ant1 is a unipolar CPW differential dual-polarization antenna, Ant2 is a slotted

CPW differential dual-polarization antenna, and Ant3 is a cross-slotted CPW differential dual-polarization antenna. It should be noted that all the three antennas in Fig. 2 have the same dimensions and the same substrate as the antenna in Fig. 1. Compared with Ant1, the ground in Ant2 is extended toward the patch direction so that the current distribution area increases and radiates with the patch, thus widening the antenna bandwidth. To obtain better impedance-matching characteristics, cross-shape slots are loaded in Ant3. Due to the symmetrical structure of these antennas, the horizontal and vertical polarization performances are basically the same. Figure 3 shows the simulation results of the three antennas in the case of vertical polarization.
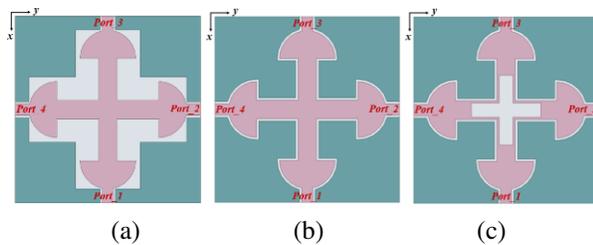
Fig. 2. Antenna design process. (a) Ant1. (b) Ant2. (c) Ant3.

The bandwidth of a traditional planar microstrip slotted antenna is narrow. By increasing the height of the dielectric plate and reducing the dielectric constant of the dielectric plate to improve the impedance bandwidth of the antenna, it may bring some problems such as stray loss, decrease of antenna efficiency, and distortion of the pattern. Therefore, Ant2 extends the ground towards the direction of the radiation patch on the basis of Ant1. This improvement can increase the current distribution area and generate a certain radiation effect, thus improving the impedance bandwidth and dual-polarization performance. To obtain better impedance matching, a cross-shape structure is etched in the center of the radiation patch to form Ant3. The loading of the cross-shape slot is equivalent to adding a series inductor to the circuit, and a new slot capacitance is created between the ground and the radiation patch. A new resonance is thus formed around the main resonance, promoting the formation of multiple resonances and effectively widening the bandwidth. Due to the cross-shape gap being a symmetrical structure, the interference to radiation pattern is small.

It can be seen from Fig. 3 that the impedance bandwidth of Ant3 is obviously better than that of the other two antennas. All three antennas have good port isolation, which is greater than 22 dB. However, Ant3 has lower port isolation and better performance compared
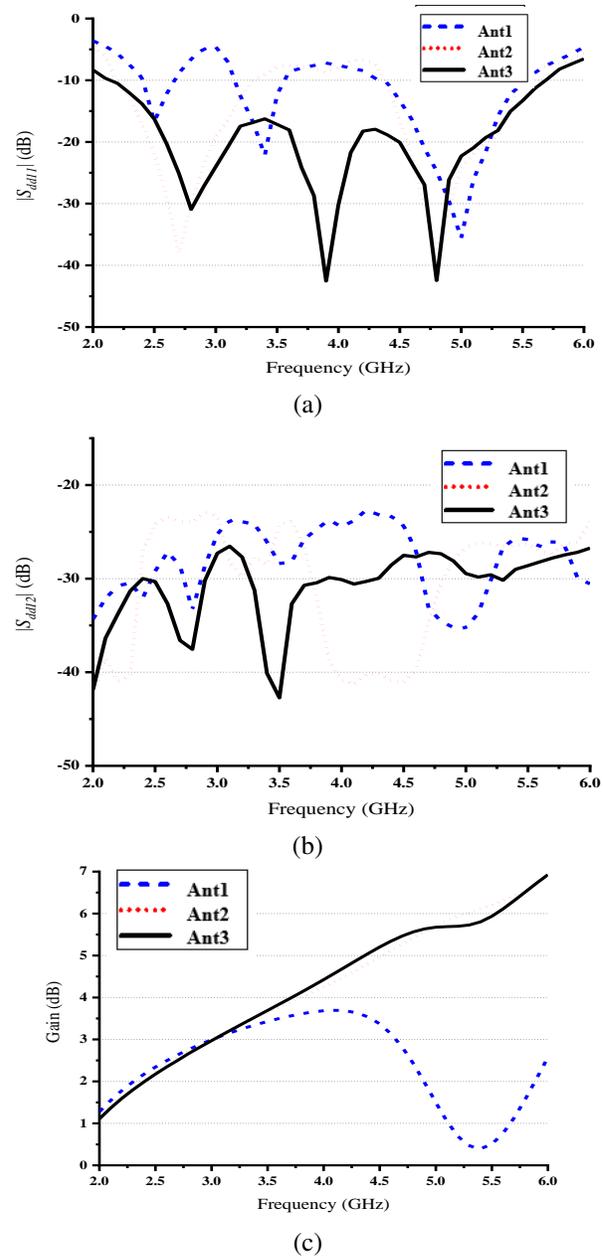
Fig. 3. Simulation results of three kinds of antennas. (a) $|S_{dd11}|$. (b) $|S_{dd12}|$. (c) Gain.

with the other two antennas. In Fig. 3 (c), the gain of Ant2 and Ant3 at high frequency is significantly higher than that of Ant1. Compared with the other two antennas, Ant3 has wider operating bandwidth, relatively higher gain and port isolation, which is the optimal antenna structure. The comparison of impedance bandwidths, isolation and peak gain variations of Ants 1-3 is listed in Table 1.

Figure 4 shows the surface current distribution of Ant3 operating at 2.3 GHz, 4.0 GHz, and 5.4 GHz. When

Table 1: Comparison of Ants 1-3

Antenna	Bandwidth	Isolation (dB)	Peak Gain (dB)
Ant1	4.31 - 5.54 GHz	>22	3.72
Ant2	4.38 - 5.53 GHz	>22	6.77
Ant3	2.27 - 5.56 GHz (82.25%)	>28	6.86

(a)   (b)   (c)
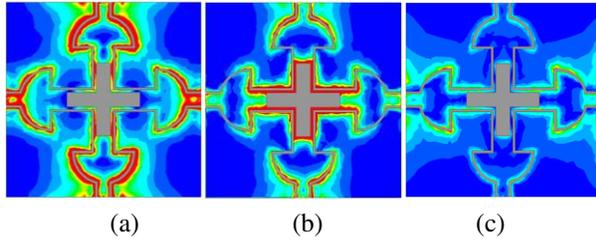
Fig. 4. Surface current distribution of Ant3 at different frequencies. (a) 2.3 GHz. (b) 4.0 GHz. (c) 5.4 GHz.

the antenna operates at 2.3 GHz, the current mainly concentrates at the edge of the semicircle radiation patch and the ground slot. At 4.0 GHz, the current mainly concentrates at the edge cross-shape slot, resulting in a new resonance point. At 5.4 GHz, the current mainly concentrates at the gap edge between the radiation patch and the ground. The length of the cross-shape slot is 76 mm, and the electric length is about $0.5\lambda_0$ (λ_0 is the wavelength at 4 GHz), which meets the condition of half wave slot, indicating that the slot works in the middle frequency band and can produce effective radiation.

C. Principle of dual-polarization generation

The antenna is excited by two pairs of differential ports through four SMA heads to generate and radiate

(a)   (b)
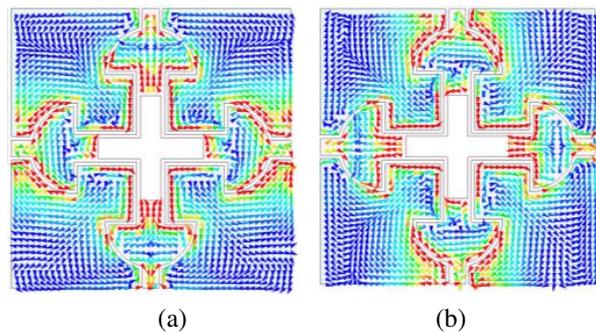
Fig. 5. Surface vector current distribution of Ant3 at 4.0 GHz. (a) Exciting Port_1 and Port_3. (b) Exciting Port_2 and Port_4.

vertically-polarized and horizontally-polarized waves. In order to verify the generation principle of dual polarization, Fig. 5 shows the vector current distribution of the antenna fed by different ports at 4 GHz. When port_1 and port_3 feed signals with equal amplitude and phase difference of 180°, port_2 and port_4 are connected with 50 Ω load. It can be seen from Fig. 5 (a) that when the electric fields of the patch in the Y direction cancel each other, leaving only the electric field in the X direction, then the antenna will generate and radiate the vertically-polarized wave. Similarly, when port_2 and port_4 feed signals with equal amplitude and phase difference of 180°, port_1 and port_3 are connected with 50 Ω load. It can be seen from Fig. 5 (b) that when the electric fields in the X direction of the patch cancel each other, leaving only the electric field in the Y direction, then the antenna will generate and radiate horizontally-polarized waves.

III. NUMERICAL RESULTS
A. Parameter analysis

According to the structure design, the size of the semicircular and the rectangular patch, the width of the feeder line, and the gap width between the ground and the patch will affect the performance of the antenna. It is therefore helpful to select the optimal size parameters for best performances by analyzing the influences of the key parameters on the performances of the antenna.

The effects of different variables on antenna performance are shown in Fig. 6. Assuming that other parameters remain unchanged, the relationship between radius R and antenna performance is analyzed in Fig. 6 (a). With the increase of R, the impedance bandwidth increases continuously. Due to the limitation of the overall size of the antenna, R chooses 6 mm as the best size. It can be seen from Fig. 6 (b) that as parameter k decreases continuously, the better the impedance- matching effect of mid-frequency part is, and the better the combination effect of multiple resonant modes is. When $p = 1.6$ mm, the resonant point of the antenna shifts to the low frequency part, which leads to poor matching of the high frequency part. When $p = 3.2$ mm, the spacing between the three resonant points becomes smaller, and the bandwidth of differential mode impedance matching becomes narrower. When $p = 2.4$ mm, the antenna gets the widest impedance-matching bandwidth. As the gap width s increases, multiple resonant points obviously move towards high frequency, which will lead to the poor matching effect of the antenna at low frequency. Considering the frequency band that the antenna needs to work, $s = 0.5$ mm is finally selected as the optimal value.

B. Simulated and experimental results

Figure 7 shows the fabricated antenna and the comparison of measured and simulated differential mode S parameters in two polarization modes. The vector

(a)

(b)

(c)

(d)
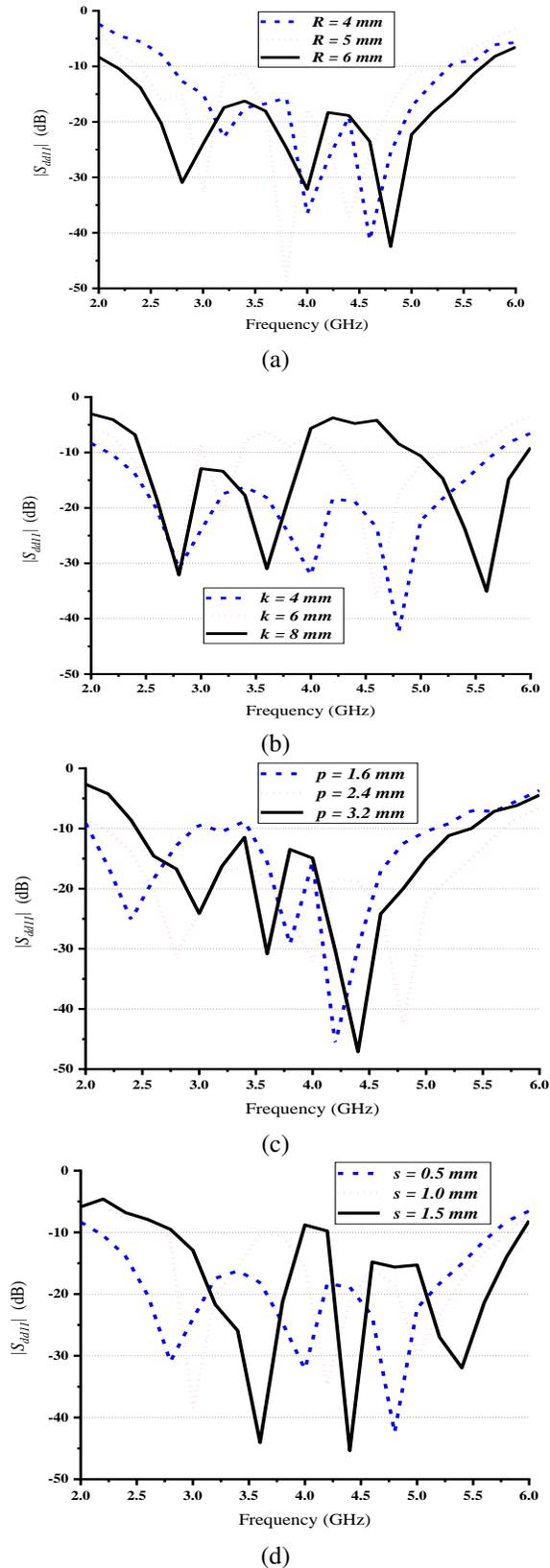
Fig. 6. Parameter study of $|S_{dd11}|$ with different dimensions as the parameter: (a) R. (b) k. (c) p. (d) s.

network analyzer Agilent is employed to measure the S-parameters. It can be seen from Fig. 7 (b) that the differential mode impedance bandwidth of the antenna is 2.27-5.56GHz, and the relative bandwidth is 82.25%. In this frequency band, the isolation of the differential port is higher than 28 dB as shown in Fig. 7 (c). The discrepancies between simulated and measured results may be due to fabrication tolerances, imperfect soldering, and measurement tolerances.

(a)

(b)

(c)
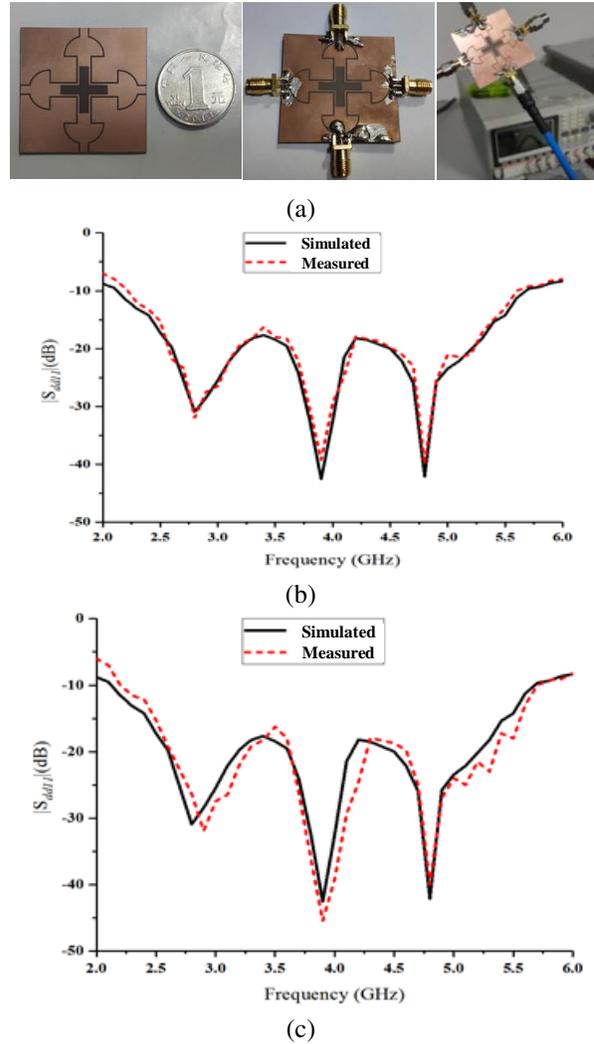
Fig. 7. Comparison of simulation and measured results. (a) Fabricated antenna. (b) Vertical polarization. (c) Horizontal polarization.

Figures 8 and 9 depict the simulated and measured radiation patterns of the proposed antenna in vertical and horizontal polarization at 2.3 GHz, 4.0 GHz, and 5.4 GHz, showing good agreement with each other. It can be seen that the cross polarization level of the antenna is extremely low within the working bandwidth, which is less than -30 dB. It has a stable radiation pattern and
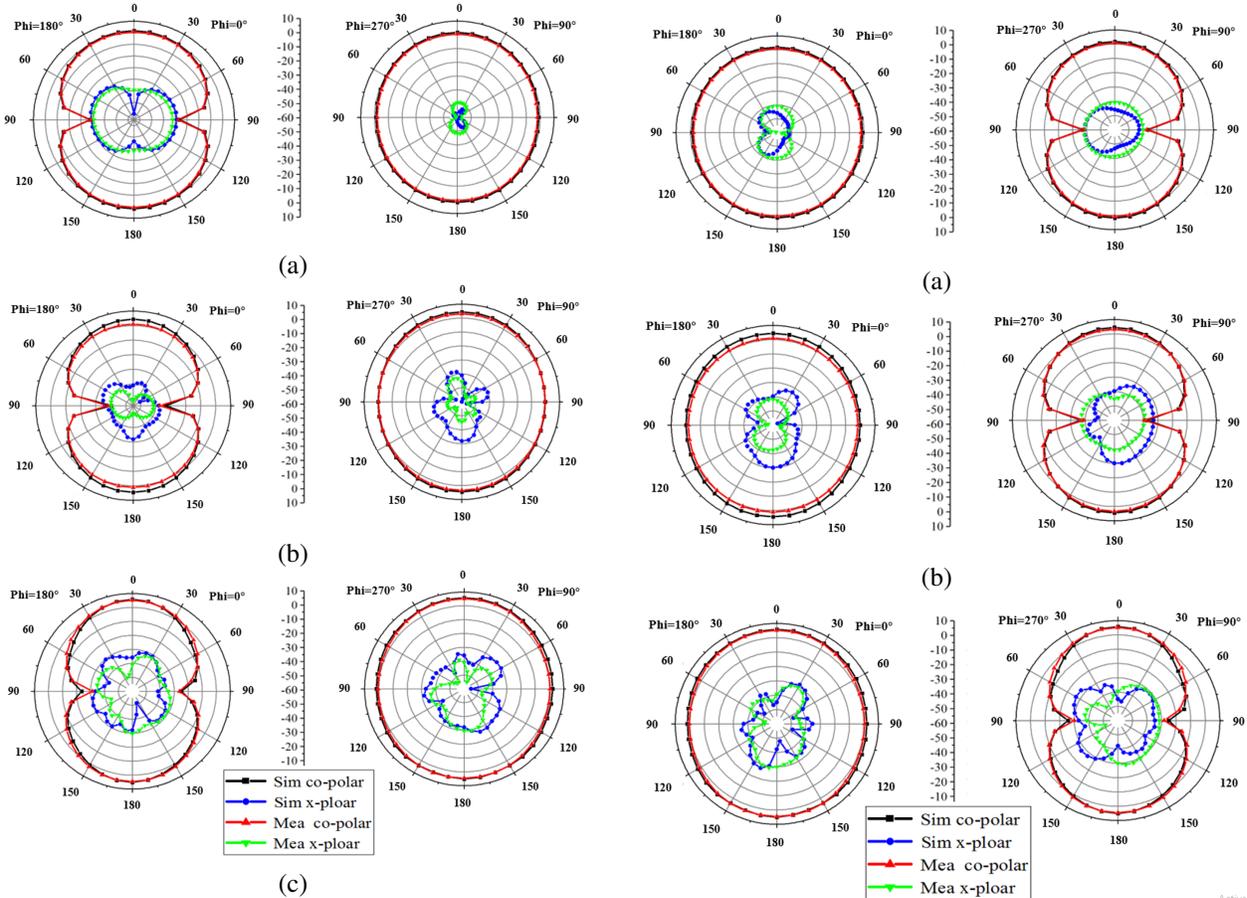
Fig. 8. Simulated and measured radiation patterns in vertical. (a) xoz and yoz plane at 2.3 GHz. (b) xoz and yoz plane at 4.0 GHz. (c) xoz and yoz plane at 5.4 GHz.

an extremely low cross polarization level. However, with the increase of frequency, the polarization isolation decreases slightly.

As the designed antenna is a dual polarization antenna, the following formula is used to calculate the radiation efficiency.

$$\text{Radiation Efficiency} = \frac{\text{Radiated Power}}{\text{Incident Power}}, \quad (2)$$

where radiated power and incident power are directly simulated by HFSS software. The simulated radiation efficiency and gain are shown in Fig. 10, where one sees that the radiation efficiency is better than 70% over the working bandwidth. As can be seen from Fig. 10, the gain is linearly increasing over the entire band, the average gain of the antenna in both polarization modes is 4.27 dB, and the maximum gain is 6.86 dB, but the gain of the low-frequency part is slightly lower.

Table 2 shows the performance comparison between the antenna proposed in this paper and the antenna in the cited literature. The results show that the antenna has
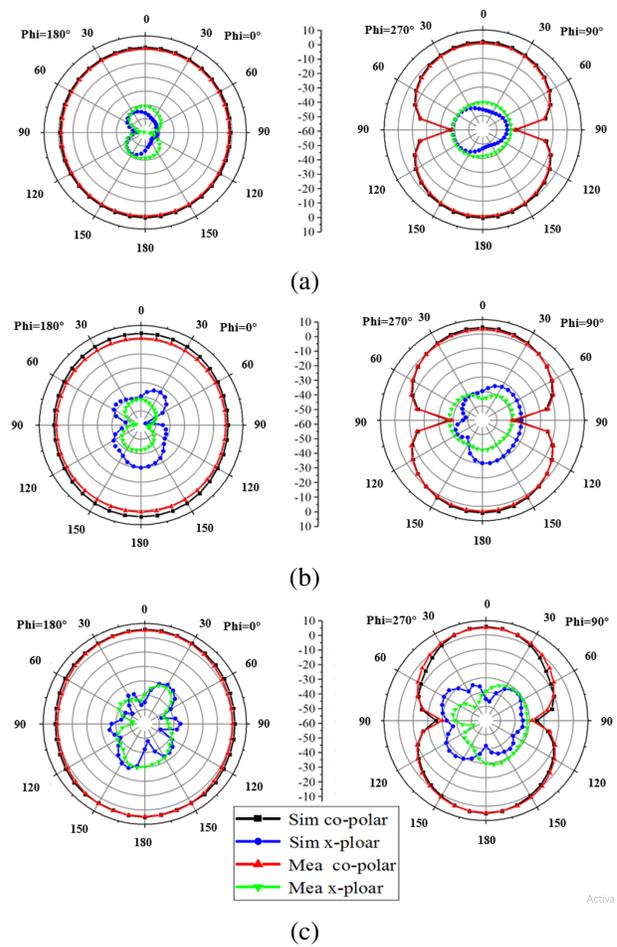
Fig. 9. Simulated and measured radiation patterns in horizontal. (a) xoz and yoz plane at 2.3 GHz. (b) xoz and yoz plane at 4.0 GHz. (c) xoz and yoz plane at 5.4 GHz.
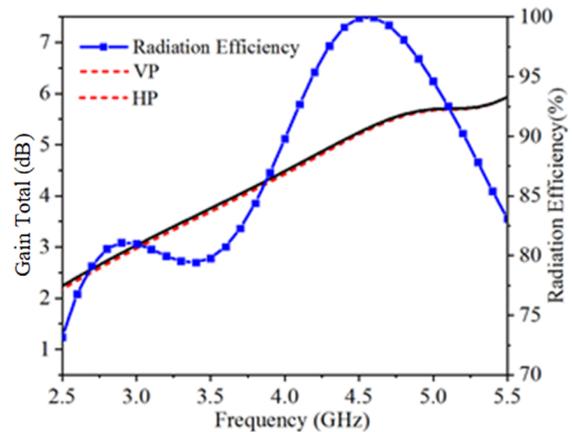
Fig. 10. Simulated radiation efficiency and gain.

a wider impedance bandwidth, a smaller relative size, a higher isolation, and a lower cross-polarization level.

Table 2: Comparison of the proposed antenna with some existing works

Ref.	Dimension	Common Bandwidth	Isolation (dB)	Cross-polarization (dB)
[11]	$0.82\lambda_0 \times 0.82\lambda_0 \times 0.27\lambda_0$		> 26	< -25
[12]	$0.46\lambda_0 \times 0.46\lambda_0 \times 0.17\lambda_0$	$0.575 - 0.722\text{GHz}$ (22.7%)	> 35	< -30
[13]	$1.1\lambda_0 \times 1.39\lambda_0 \times 0.13\lambda_0$	$1.67 - 2.98\text{GHz}(56\%)$	> 25	< -20
[14]	$1.23\lambda_0 \times 1.23\lambda_0 \times 0.0075\lambda_0$	$1.70 - 2.71\text{GHz}(45.8\%)$	> 33	< -20
[15]	$0.49\lambda_0 \times 0.71\lambda_0 \times 0.0034\lambda_0$	$1.63 - 2.93\text{GHz}$ (57%)	> 32	< -15
This paper	$0.53\lambda_0 \times 0.53\lambda_0 \times 0.0135\lambda_0$	$2.27 - 5.56\text{GHz}$ (82.25%)	> 28	< -30

IV. CONCLUSION

In this paper, a compact ultra-wideband dual-polarization planar slotted antenna has been designed, optimized and fabricated. It consists of a mushroom-shaped radiation patch and a ground surface, both of which form a gap and are located above the dielectric substrate. Coplanar waveguide structure is used for differential feed to suppress cross polarization. By extending the ground to the patch direction and loading a cross-shape slot in the middle of the radiation patch, the operating frequency band of the antenna is effectively widened. The simulated and measured results show that the relative bandwidth of the proposed antenna is 82.25% ($2.27 \sim 5.56$ GHz), the cross polarization is less than -30 dB, and the port isolation is higher than 28 dB. The proposed antenna, with a height of $0.0135\lambda_0$ (where λ_0 is the free-space wavelength at central frequency 4 GHz), has the advantages of easy fabrication, stable radiation, and low cross polarization, so it is suitable for dual polarization communication systems.

ACKNOWLEDGEMENTS

REFERENCES

[1] P. Qin, L. Ji, S. Chen, and Y. J. Guo, "Dual-polarized wideband Fabry–Perot antenna with quad-layer partially reflective surface," *IEEE Antennas Wirel. Propag. Lett.*, vol. 17, no. 4, pp. 551-554, Feb. 2018.

[2] Z. Tang, J. Liu, R. Lian, Y. Li, and Y. Yin, "Wideband differentially fed dual-polarized planar antenna and its array with high common-mode suppression," *IEEE Trans. Antenn. Propag.*, vol. 67, no. 1, pp. 131-139, Oct. 2019.

[3] B. Peng, S. Li, J. Zhu, L. Deng, and Y. Gao, "A compact wideband dual-polarized slot antenna with five resonances," *IEEE Antennas Wirel. Propag. Lett.*, vol. 16, pp. 2366-2369, June 2017.

[4] Y. Chen, W. Lin, S. Li, and A. Raza, "A broadband $\pm 45°$ dual-polarized multidipole antenna fed by capacitive coupling," *IEEE Trans. Antenn. Propag.*, vol. 66, no. 5, pp. 2644-2649, Feb. 2018.

[5] H. Jin, L. Zhu, H. Zou, Y. Luo, S. Xu, and G. Yang, "A wideband dual-polarized antenna and its array with electrically downtilt function for 5G sub-6 GHz communication applications," *IEEE Access*, vol. 8, pp. 7672-7681, Dec. 2020.

[6] Y. Li, C. Wang, and Y. X. Guo, "A Ka-Band wideband dual-polarized magnetoelectric dipole antenna array on LTCC," *IEEE Trans. Antenn. Propag.*, vol. 68, no. 6, pp. 4985-4990, Nov. 2020.

[7] D. Zheng and Q. Chu, "A wideband dual-polarized antenna with two independently controllable resonant modes and its array for base-station applications," *IEEE Antennas Wirel. Propag. Lett.*, vol. 16, pp. 2014-2017, Apr. 2017.

[8] H. Tang, J. Chen, W. Yang, L. Zhou, and W. Li, "Differential dual-band dual-polarized dielectric resonator antenna," *IEEE Trans. Antenn. Propag.*, vol. 65, no. 2, pp. 855-860, Nov. 2017.

[9] Z. Zhang and K. Wu, "A wideband dual-polarized dielectric magnetoelectric dipole antenna," *IEEE Trans. Antenn. Propag.*, vol. 66, no. 10, pp. 5590-5595, July 2018.

[10] L. Wen, S. Gao, Q. Luo, Q. Yang, W. Hu , Y. Yin, X. Ren, and J. Wu, "A compact wideband dual-polarized antenna with enhanced upper out-of-band suppression," *IEEE Trans. Antenn. Propag.*, vol. 67, no. 8, pp. 5194-5202, May 2019.

[11] C. Zhou, H. Wong, and L. K. Yeung, "A wideband dual-polarized inductor-end slot antenna with stable beamwidth," *IEEE Antennas Wirel. Propag. Lett.*, vol. 17, no. 4, pp. 608-612, Feb. 2018.

[12] S. Zhou, P. Tan, and T. Chio, "Low-profile, wide-band dual-polarized antenna with high isolation and low cross polarization," *IEEE Antennas Wirel. Propag. Lett.*, vol. 11, pp. 1032-1035, Aug. 2012.

[13] Y. Zhang, "Wideband Low-Profile Dual-Polarized Antenna," Harbin Institute of Technology, June 2019.

[14] S. Jamilan, M. A. Antoniades, J. Nourinia, and M. N. Azarmanesh, "A directivity-band-dependent triple-band and wideband dual-polarized monopole antenna loaded with a via-free CRLH unit cell," *IEEE Antennas Wirel. Propag. Lett.*, vol. 14, pp. 855-858, Dec. 2015.

[15] B. Peng, S. Li, J. Zhu, L. Deng, and Y. Gao, "A compact wideband dual-polarized slot antenna with five resonances," *IEEE Antennas Wirel. Propag. Lett.*, vol. 16, pp. 2366-2369, 2017.

[16] Y. Liu and Z. Tu, "Compact differential band-notched stepped-slot UWB-MIMO antenna with common-mode suppression," *IEEE Antennas Wirel. Propag. Lett*, vol. 16, pp. 593-596, July 2017.

[17] Z. Tang, J. Liu, R. Lian, Y. Li, and Y. Yin, "Wideband differentially fed dual-polarized planar antenna and its array with high common-mode suppression," *IEEE Trans. Antenn. Propag.*, vol. 67, no. 1, pp. 131-139, Oct. 2019.

Zhao Neng Jiang was born in Jiangsu, China. He received the Ph.D. degree from Nanjing University of Science and Technology, Nanjing, China, in 2012. Since 2013 he has worked on numerical methods of computational electromagnetism. His current focus is on antenna and microwave devices. (Email: jiangzhaoneng@hfut.edu.cn)

Zhi Xin Wang was born in Anhui, China, in 1998. She is currently working towards the M.E. degree in Computer and Information Engineering from Hefei University of Technology. Her current focus is on antenna and microwave device design. (Email: 1364665074@qq.com)

Xiao Feng Xuan was born in Anhui, China, in 1975. He received the M.S. degree from Nanjing University, China. His focus is on numerical methods of computational electromagnetism. (Email: 941067868@qq.com)

Li Ying Nie (corresponding author) received the Ph.D. degree from the University of Electronic Science and Technology of China. Her focus is on the theory and design of microwave and millimeter wave antenna. (Email: liyingnie@sina.com)

Ye Jiang received the B.Sc. and M.Sc. degrees in Communication Engineering from China University of Mining and Technology, Xuzhou, China, in 2010 and 2013 respectively. And the Ph.D. degree in Communication and Information System from University of Chinese Academy of Science, Shanghai, China, in 2017. She is a lecture with the School of Computer Science and Information Engineering, Hefei University of Technology, Hefei, China. Her current research interests include artificial intelligence technology and intelligence computation. She has published over 10 refereed articles.